ResearchSpace@Auckland

Suggested Reference

Shafaei, J., Hosseini, A., Marefat, M. S., & Ingham, J. M. (2014). Rehabilitation of earthquake damaged external RC beam-column joints. In *Towards Integrated Seismic Design* (pp. 10 pages). Auckland. Retrieved from http://db.nzsee.org.nz/2014/Orals.htm

Copyright

Rehabilitation of earthquake damaged external RC beam-column joints

J. Shafaei, A. Hosseini & M. S. Marefat

School of Civil Engineering, College of Engineering, University of Tehran, Tehran, Iran.

J. M. Ingham

Department of Civil & Environmental Engineering, University of Auckland, Auckland, New Zealand.

2014 NZSEE Conference

ABSTRACT: Post-earthquake inspections of damaged RC buildings have demonstrated that poorly detailed beam-column joints can suffer serious damage. The effectiveness of a rehabilitation method based on joint enlargement using prestressed steel angles to enhance the seismic behaviour of damaged external reinforced concrete beam-column joints was experimentally investigated. Three half scale external RC beam-column joints with seismic and non-seismic reinforcement details were tested before and after rehabilitation by applying lateral cyclic loading of increasing amplitudes. Tested specimens were comprised of one unit having seismic reinforcement detailing and two units having non-seismic reinforcement detailing. Two defects were considered for the non-seismic units, being the absence of transverse steel hoops and insufficient bond capacity of beam bottom steel reinforcing bars in the joint panel zone. The damaged specimens were rehabilitated by injecting epoxy grout into existing cracks and installing stiffened steel angles at the re-entrant corners of the beam-column joint, both above and below the beam, that were mounted and held in place using prestressed high tensile strength bars. The test results indicated that the seismic performance of the rehabilitated specimens, in terms of strength, stiffness and ductility were fully recovered with respect to the performance of the seismically detailed specimen in the initial loading.

1 INTRODUCTION

Recent earthquakes in New Zealand, and particularly the 22 February 2011 Christchurch earthquake, caused numerous fatalities and financial losses due to the failure of reinforced concrete (RC) structures (Elwood *et al.* 2012, Kam *et al.* 2011). Post-earthquake inspections of damaged RC buildings (Dogangun 2004, Korkmaz and Korkmaz 2013, Norton *et al.* 1994, Ozturk 2013) as well as laboratory tests of non-seismic RC beam-column joints (Cheung *et al.* 1991, Leon and Jirsa 1986, Park 2002) have demonstrated that beam-column joints suffered serious damage because of deficient reinforcement details in the joint region. Failure in the beam-column joints can be primarily attributed to the absence of transverse reinforcement and insufficient bond length of the beam bottom bars in the joint panel zone, which increases the seismic vulnerability of the structures (Engindeniz *et al.* 2005). The failure of non-seismically detailed beam-column joints during past earthquakes opened a new research direction in the field of repair and improvement of damaged beam-column joints. By considering the commonly accepted idea that failure of joints may quickly lead to general failure of a structure (Park and Paulay 1975, Paulay and Priestley 1992), the important issue of determining effective methods for repair and improvement (rehabilitation) of damaged RC beam-column joints has arisen.

Several retrofit techniques for deficient RC beam-column joints have been studied in the past. Sugano (1996) presented an overview of seismic retrofitting techniques for existing pre-1970s buildings and Engindeniz *et al.* (2005) studied the efficiency of various rehabilitation technique for non-seismically detailed RC beam-column joints. From this review it can be concluded that issues of cost, invasiveness, and practical implementation still remain the most challenging aspects of rehabilitation techniques. A retrofit technique called "joint enlargement using prestressed steel angles" was experimentally investigated and found to be a simple, low-invasive, practical and cost-effective

technique for seismic retrofit of non-seismically detailed RC beam-column joints (Shafaei *et al.* 2013, Shafaei *et al.* 2012). In the current experimental investigation a combination of two repair methods that according to FEMA 308 (1998) recommendations are classified as "epoxy injection" and "removal and replacement" and a retrofit method called "joint enlargement using prestressed steel angles" were used to repair and improve the performance of beam-column joints damaged due to cyclic deformations. Three half scale external RC beam-column joint with seismic and non-seismic reinforcement details were tested before rehabilitation by applying lateral cyclic loading of increasing amplitudes and then the damaged specimens were rehabilitated by injecting epoxy grout into existing cracks and installing stiffened steel angles at the re-entrant corners of the beam-column joint, both above and below the beam, that were mounted and held in place using prestressed high tensile strength bars. The rehabilitated joints were then retested.

2 EXPERIMENTAL PROGRAM

The experimental program consisted of three half scale external RC beam-column joints with seismic and non-seismic reinforcement details and identical dimensions, which were tested before and after rehabilitation by applying lateral cyclic loading of increasing amplitudes. Tested specimens were comprised of one unit having seismic reinforcement detailing and two units having non-seismic reinforcement detailing. Two defects were considered for the non-seismic units, being the absence of transverse steel hoops and insufficient bond capacity of beam bottom steel reinforcing bars in the joint region. The damaged specimens were rehabilitated by injecting epoxy grout into existing cracks and installing stiffened steel angles at the re-entrant corners of the beam-column joint, both above and below the beam, which were mounted and held in place using prestressed high tensile strength bars. Specimen C1 represented a seismic beam-column joint designed to satisfy ACI Committee 318M-11 (2011) requirements as a benchmark specimen, whereas specimens C2 and C3 had inadequate reinforcement detailing in the joint region and represented RC structural sub-assemblies having deficient detailing. Specimens RC1, RC2 and RC3 represented rehabilitated external beam-column joint specimens. The dimensions and reinforcement details of the control specimens are shown in **Figure 1**.
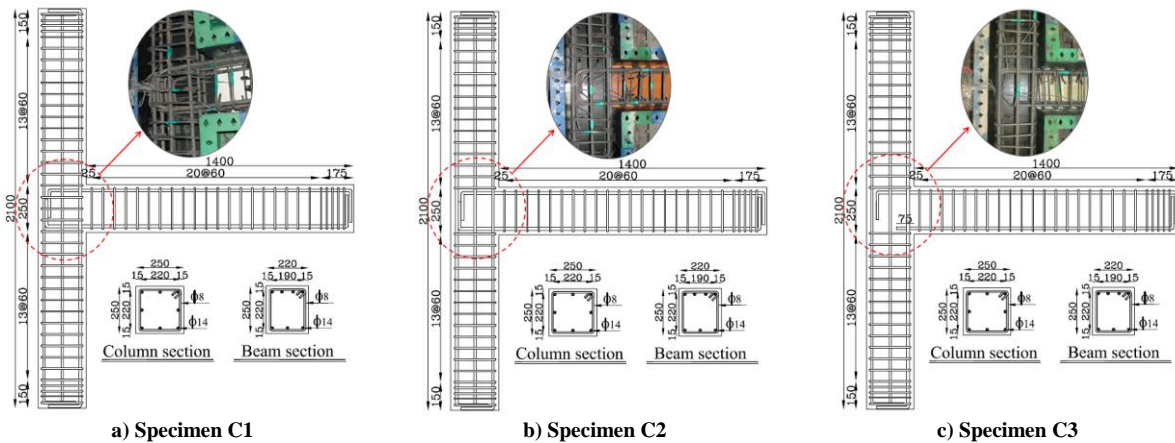

a) Specimen C1   b) Specimen C2   c) Specimen C3

Figure 1. **Dimensions and reinforcement details of control specimens (dimensions in millimetres).**

2.1 Descriptions of control specimens

Dimensions and reinforcement details of all control specimens were identical except for the reinforcement details in the joint region as shown in **Figure 1**. The column height and beam length represented the distance to the points of contraflexure for seismic bending moments. The column height was 2100 mm with cross section dimensions of 250×250 mm and the beam length was 1400 mm from the face of the column to its free end, with a cross section of 220×250 mm. The longitudinal reinforcement used in the column was 8ϕ14 deformed bars, corresponding to a 2% reinforcement ratio and the transverse reinforcement in the column was ϕ8 deformed bars with 135° end hooks that were spaced at 60 mm inside and outside the joint panel zone. The top and bottom longitudinal reinforcement of the beam were 4ϕ14 and 3ϕ14 deformed bars, corresponding to a 1.22%

2

and 0.91% reinforcement ratio respectively, and the transverse reinforcement of the beam was φ8 rectangular ties starting at 25 mm from the face of the column that were spaced at 60 mm for the beam length. The longitudinal and transverse reinforcement of all control specimens for the beam and column satisfied ACI 318M-11 seismic requirements (see **Figure 1**). Specimen C1 had sufficient shear reinforcement in the joint, while specimen C2 was designed as a shear-deficient specimen provided with no transverse shear reinforcement in the joint region and specimen C3 was designed as a shear-deficient and anchorage critical specimen with the bottom longitudinal reinforcement in the beam anchored 75 mm from the column face and with no transverse reinforcement installed in the joint region. The dimensions and joint reinforcement details of the control specimens C1, C2 and C3 are shown in **Figure 1**.

2.2 Material properties of concrete and steel reinforcement

All test specimens were constructed using normal weight and ready mixed concrete with targeted 28-day concrete compressive strength of 23 MPa and concrete specified slump of 80 mm, with maximum aggregate size of 19 mm. Each entire specimen was cast as a single element lying horizontally on the laboratory floor and was wet-cured for 7 days. Yield strength of the steel reinforcement for 8 mm and 14 mm diameters was 350 MPa and 460 MPa respectively.

2.3 Test setup and instrumentation

The test setup with the specimen supports and other key components is illustrated in **Figure 2**. All specimens were tested with the column positioned horizontally and the beam standing vertically, thereby being rotated 90-degree from the true orientation. Roller supports were constructed and the top of the beam was linked to an actuator with a swivel connector to simulate the support condition at the top of the beam and both ends of the column. Thus the top of the beam and the left and right of the column were all pin-connected in the loading plane, to simulate the inflection points of a moment frame subjected to lateral earthquake loading.
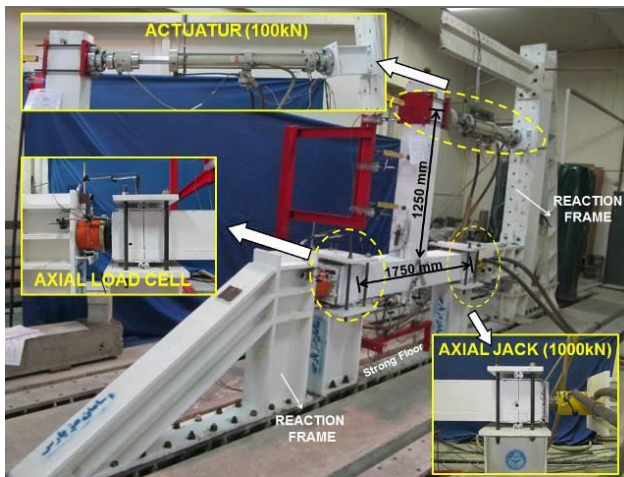

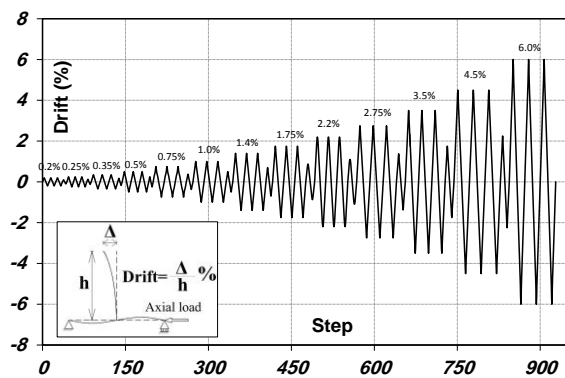**Figure 2**. **View of test setup.**

Figure 3. **Lateral cyclic loading protocol.**

Lateral cyclic loading with increasing amplitudes was statically applied to the top of the beam in two opposite directions, parallel to the longitudinal direction of the column, by a hydraulic actuator with a ±100 kN loading capacity and a ±200 mm displacement range, and a horizontal 1000 kN capacity hydraulic jack was used to apply constant axial load to the column to simulate gravity actions. The position of the hydraulic jack, axial jack and load cell are indicated in **Figure 2**. The two ends of the column were restrained against both vertical and horizontal deformations, whereas their rotations were allowed due to the hinged boundary conditions.

2.4 Test procedure and Loading characteristics

For both control and rehabilitated specimens a constant axial load of 220 kN (16% of the column axial capacity) was applied to the column in a force controlled mode and was maintained constant

throughout each test. After application of the 220 kN axial load to the end of the column, low rate lateral cyclic loading of increasing amplitudes was applied at the top of the beam in a displacement controlled mode to identify the cyclic behaviour of the beam-column joint. The loading procedure for all specimens was based on acceptance criteria specified in ACI Committee 374.1-05 (2005) utilizing displacement (drift) control to preliminary target drifts. **Figure 3** shows the lateral cyclic loading protocol according to ACI 374.1-05.

2.5 Seismic behaviour and failure modes of control specimens

The damage pattern of control specimens at the end of testing are shown in Figure 4, illustrating that specimen C1 was controlled by the flexural mechanism of the beam at the beam-column interface, whereas specimens C2 and C3 failed by concrete crushing in the joint region. The first flexural cracks of all control specimens appeared at the bottom of the beam at 0.25% drift, and for specimens C1 and C2 these cracks gradually propagated to a height of 750 mm whereas for specimen C3 these cracks propagated to a height of 300 mm for the pull direction, and to 650 mm for the push direction. Yield of longitudinal and transverse reinforcement was measured by strain gauges, with first yield of the beam longitudinal reinforcement occurring at a drift ratio of 1.1% for specimen C1, while yield of the beam longitudinal reinforcement was not recorded for specimens C2 and C3.

For specimen C1, spalling of concrete cover at the column surface commenced at a drift ratio of between 1.75 to 2.2%, and diagonal cracking in the joint zone began at a drift of 1.75% for the push direction. Additional cracking in the joint panel zone appeared thereafter as loading progressed, but crack widths remained fine throughout the test. At a drift ratio of 3.5% the beam became extensively cracked along a distance equal to its depth from the column face, and at a drift ratio of 4.5% wide cracks developed in the beam potential plastic hinge zone and spalling commenced, as shown in Figure 4a.

For Specimen C2, X-shape cracks in the joint panel zone commenced at a drift ratio of 0.75%, indicating imminent joint failure. The flexural and diagonal cracks grew in size and number as the drift ratio increased. Spalling of concrete cover appeared in the joint region at a drift ratio of between 1.4 to 2.0%, and from a drift of 2.0% the cracking was mainly concentrated in the joint region and formed a typical X-shaped pattern, as shown in Figure 4b. At a drift ratio of 3.5% the concrete in the joint panel zone spalled and crushed, exposing the column longitudinal reinforcement. Lateral cyclic loading was continued with substantial damage in the joint panel zone until 4.5% drift, as shown in Figure 4b.

| a) Specimen C1 | b) Specimen C2 | c) Specimen C3 |

Figure 4. Damage pattern of control specimens C1, C2 and C3 at the end of testing.

For specimen C3 the vertical cracks in the joint panel formed at a drift ratio of 0.5%, due to bond-slip of the beam bottom reinforcement for the pull direction, and diagonal shear cracks in the joint zone developed at a drift ratio of 0.75% for the push direction. When the specimen was next loaded in the opposite direction the bond-slip cracks opened and the lateral load-carrying capacity deteriorated significantly, and then when reversed back the diagonal shear cracks in the joint panel zone opened, causing crushing of the concrete, deterioration of the bond condition of the beam bottom reinforcement, and degradation of the lateral load-carrying capacity. Specimen C3 reached a maximum load of 20.0 kN for the pull direction, and a maximum load of 35.0 kN for the push

direction, which was much less than the strength calculated for yielding of the beam longitudinal reinforcement of 32.0 kN and 41.5 kN for the pull and push direction respectively (see Figure 4c). The test was stopped at a displacement of 54 mm, corresponding to a drift of 4.5%, as the load-carrying capacity was greatly reduced.

2.6 Proposed repair and improvement (rehabilitation) procedure of the damaged specimens

The major objective of the proposed rehabilitation procedure was to restore the lost capacity of the damaged beam-column joints to their respective original seismic capacity and prevent damage inside the joint region. All repair and improvement (rehabilitation) steps were performed at the deformed position, as discussed below.
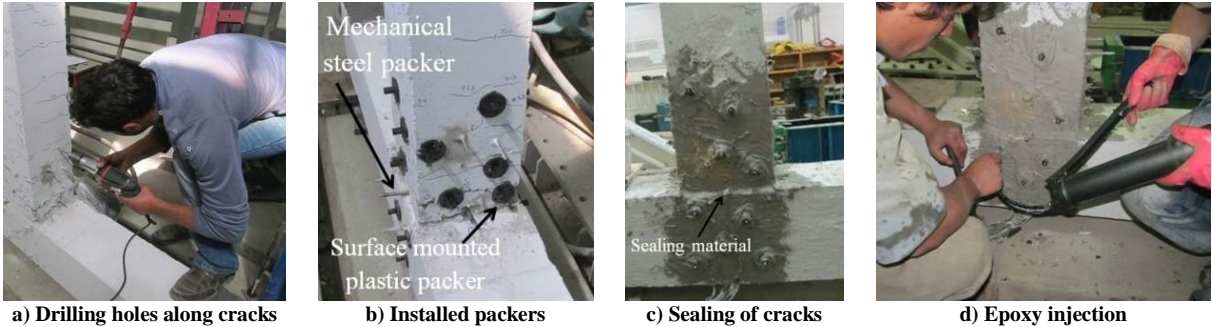

| a) Drilling holes along cracks | b) Installed packers | c) Sealing of cracks | d) Epoxy injection |

Figure 5. Step by step repair procedure#1 for specimen C1.

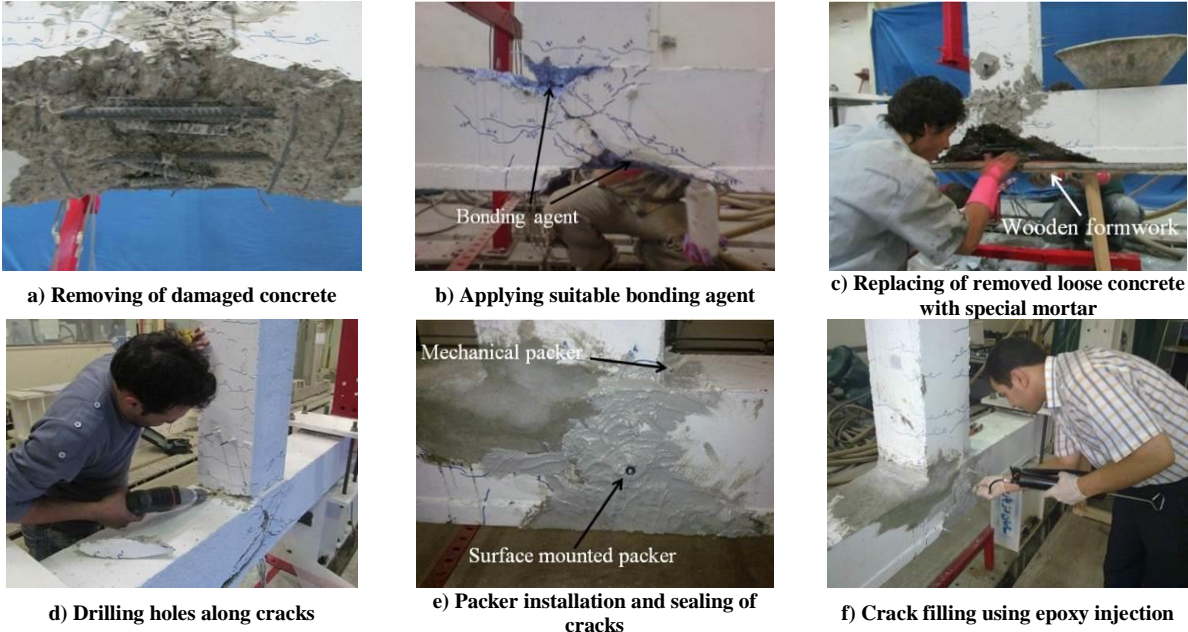| a) Removing of damaged concrete | b) Applying suitable bonding agent | c) Replacing of removed loose concrete with special mortar |
| d) Drilling holes along cracks | e) Packer installation and sealing of cracks | f) Crack filling using epoxy injection |

Figure 6. Step by step repair procedure#2 for specimens C2 and C3.

2.6.1 *Repair procedure for damaged control specimens*

The control specimens damaged due to applying lateral cyclic loading were cleaned and made ready for the repair procedure. First, loose and damaged concrete pieces were removed from all parts of the damaged specimens using a hammer and chisel and concrete surfaces were cleaned using a blower to eliminate surface dust. According to FEMA 308 recommendation, in the current study two repair procedures were employed depending on the different levels of damage. The first procedure was referred to as repair procedure#1 and as shown in **Figure 5** entailed partial replacement of loose concrete on the damaged area by special mortar, followed by epoxy injection into the cracked zone. The second procedure was referred to as repair procedure#2 and as shown in **Figure 6** entailed complete replacement of crushed concrete in the damaged area by application of special mortar, followed by epoxy injection into the cracked zone. Repair procedure#1 was applied on specimen C1

where damage was typically confined to the cover concrete of the joint region as the core concrete was confined by adequate reinforcement inside the joint and was mostly intact, whereas repair procedure#2 was applied on specimens C2 and C3 where the concrete cover and core of the joint region were seriously fragmented and complete removal of concrete from the effected zone was necessary. **Figure 5** and **Figure 6** illustrate various steps of the repair operations for damaged control specimens for the repair procedure#1 and repair procedure#2 respectively.

After the removal of loose material a bonding agent (SikaCem Concentrate) was applied on the cleaned surfaces to improve the bond between the fresh mortar and existing concrete and to increase surface hardness and significantly reduce the problem of surface dusting (see Figure 6b). A premixed, non-shrink, and self-compacting high strength mortar (Sika MonoTop-438 R) with 2.0 mm maximum aggregate size was used to replace the removed concrete and for the filling of cavities. Wooden formwork was placed on the bottom of specimens C2 and C3 where extensive repair and complete replacement of crushed concrete in the joint region was needed (see Figure 6c). Mortar was placed by hand and the surfaces of the repaired areas were made smooth by hand using a rubbing stone. The repaired areas were covered by plastic and cured for 3 days to maintain non-shrink characteristics of the new mortar. The formwork was removed after 1 week of curing.

There are two primary categories of packers for epoxy injection into cracks, namely mechanical steel packers that are used for epoxy injection into deep cracks and surface mounted plastic packers that are used for epoxy injection into shallow cracks. In the adopted repair procedure both types of packers were used. For epoxy injection into cracks, holes were drilled along cracks at pre-determined locations in the beam potential plastic hinge zone and joint panel zone (see Figure 5a and Figure 6d) and mechanical packers were inserted through these holes, which served as a filler neck for epoxy injection as shown in Figure 5b and Figure 6e. Visible cracks were sealed by high strength rigid two-part epoxy adhesive (Sikadur-31 CF Normal) as shown in Figure 5c and Figure 6e and a high-strength, high-modulus, low-viscosity epoxy resin (Sikadur-52) that filled all cracks larger than 0.3 mm was injected into the cracked zone by a hand operated injection pump (see Figure 5d and Figure 6f). Once the injected epoxy resin attained sufficient strength, the installed packers were removed by striking their head and a grinding machine was subsequently used to remove the sealing materials.

2.6.2 *Improvement procedure for repaired control specimens*

Details of the improvement procedure were the same for all repaired specimens, as shown in **Figure 7**. For all rehabilitated specimens, the total joint width including the steel angles and plates was 350 mm, which was greater than the width of the beam and column and allowed the prestressed bars to pass outside the beam and column without requiring holes to be drilled through the beam-column joint. The three steel elements that comprised the improvement intervention were held and fixed in place using high tensile strength M16 bars, washers and nuts and were prestressed until a tension force approximately equal to 70 percent of the minimum tensile strength ($0.7f_{pu}$) was produced in the bars. The length and specified ultimate tensile strength of the prestressed bars were 400 mm and 1000 MPa respectively. Tightening was achieved using a calibrated wrench and the tension in all bolts was checked by a repeat pass to ensure that all bolts were prestressed to the prescribed value. The improvement procedure adopted for repaired beam-column joints involving a steel angle size of 180 mm×180 mm×18 mm and a plate length of 610 mm. Views of the repaired control specimens RC1, RC2 and RC3 after the improvement procedure are shown in **Figure 7**.

2.7 **Seismic behaviour and failure modes of rehabilitated specimens**

The damage pattern of rehabilitated specimens at the end of testing are shown in **Figure 8**, illustrating that an almost regular and consistent pattern of cracks was observed in all rehabilitated specimens, and that the flexural mechanism in the beam at the edge of the steel angles was the failure mode for all rehabilitated beam-column joints. In **Figure 8** the blue lines show cracking patterns of control specimens before rehabilitation and red lines show cracking patterns of rehabilitated specimens after the rehabilitation procedures. The first flexural cracks for all rehabilitated specimens were observed at the edge of the joint enlargement in the beam at a drift ratio of approximately 0.2% and gradually

extended to the whole length of the beam. From cyclic testing of the control specimens it was observed that all of the strain gauges on the stirrups and longitudinal bars in the column and beam had failed. Thus, first yield of the beam longitudinal reinforcement was not able to be recorded during cyclic testing of the rehabilitated specimens. As the applied drift increased, spalling of concrete cover at the corners of the beam section and at the edge of the steel angles commenced at a drift ratio of between 1.75% to 2.20% for all rehabilitated specimens. As testing continued, damage extended towards the middle of the beam section and penetrated into the concrete core. In specimen RC1, RC2 and RC3, despite the corresponding performance of the control specimens (C1, C2 and C3), no diagonal cracks formed in the joint panel zone up to the end of testing. The behaviour of all rehabilitated specimens was generally close to each other in terms of cracking development and failure mode.
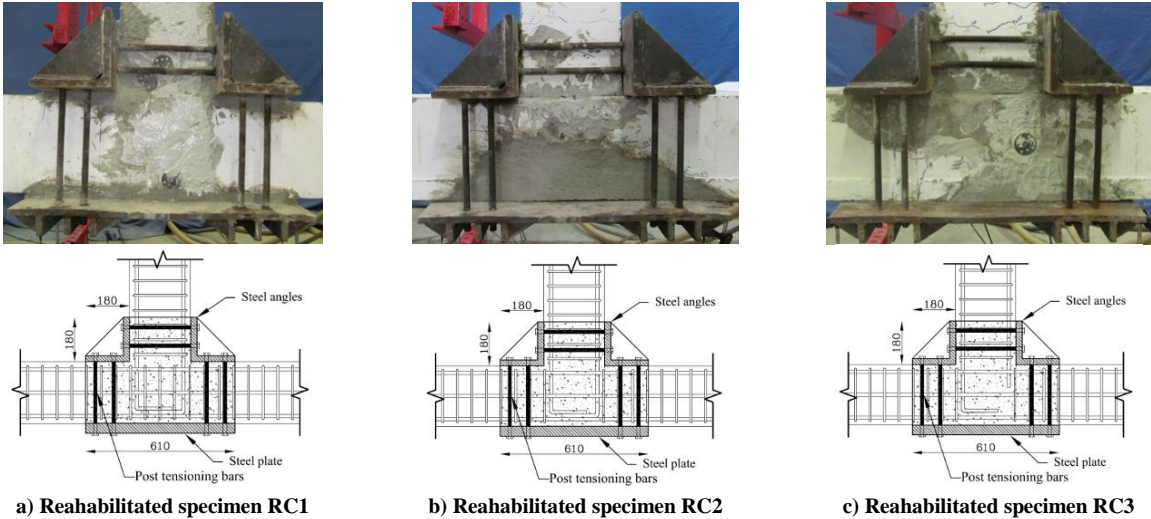

| a) Reahabilitated specimen RC1 | b) Reahabilitated specimen RC2 | c) Reahabilitated specimen RC3 |

Figure 7. Details and view of specimens after improvement (dimensions in millimetres).

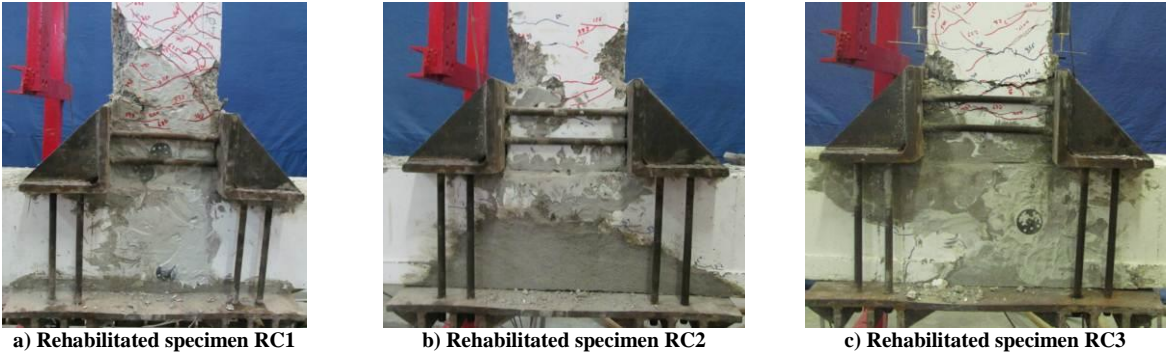| a) Rehabilitated specimen RC1 | b) Rehabilitated specimen RC2 | c) Rehabilitated specimen RC3 |

Figure 8. Damage pattern of rehabilitated specimens at the end of testing.

3 RESULTS AND DISCUSSION

3.1 Load-displacement hysteretic response of specimens

Load-displacement (and drift ratio) hysteretic response and their associated envelope curves for peak displacement points at first reversal of cycles (Elwood *et al.* 2007) are shown for the control and rehabilitated specimens in **Figure 9**. **Figure 9**a illustrates that the response of Specimen C1, the beam-column joint designed according to ACI 318M-11, exhibited ductile load-displacement hysteretic response with no notable pinching or strength drop at the end of testing. The hysteretic loops of the non-seismic specimens (C2 and C3) show considerable pinching and continuous stiffness and strength degradation with increasing displacement with respect to the seismic specimen (C1), which is

primarily attributed to the joint shear failure of specimen C2 (see **Figure 9**c) and joint shear failure and bond failure of beam bottom reinforcement of specimen C3 (see **Figure 9**e). Load-displacement hysteretic response of rehabilitated specimens RC1, RC2 and RC3 are shown in **Figure 9**b, **Figure 9**d and **Figure 9**f respectively. The hysteresis loops of the rehabilitated specimens are larger and remained stable without apparent strength deterioration and stiffness degradation with respect to their corresponding control specimens. The hysteretic response of the rehabilitated and control specimens show that the ultimate load and deformation capacity of the rehabilitated specimens was higher than their respective control specimens, for both the push and pull directions. Finally it can be concluded that the proposed rehabilitation method was effective in significantly improving the performance of the non-seismically detailed beam-column joints.
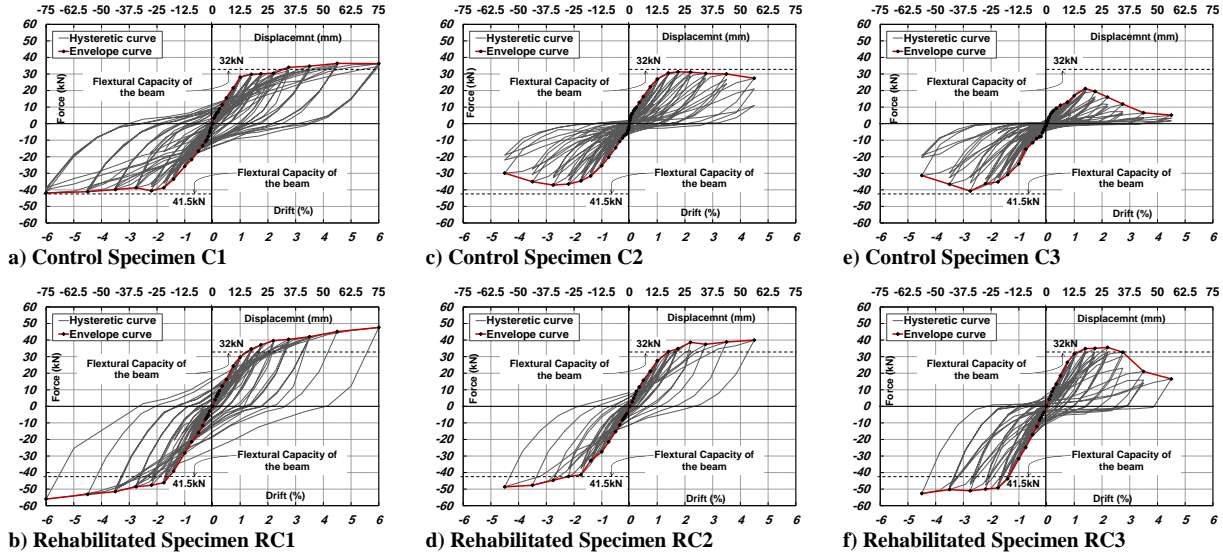

Figure 9. Load-displacement hysteretic response of control and rehabilitated specimens.

3.2 Load-displacement envelope curves

Using envelope curves, as shown in **Figure 9**, the peak load, ultimate displacements and ductility capacity for the control and rehabilitated specimens, for both the positive and negative loading direction, were obtained as reported in Table 1. The results presented in Table 1 show that there was a considerable difference in the ductility and peak load values for both pull and push directions between the control and rehabilitated specimens. The ductility values clearly show that application of the proposed method improved the ductility of the rehabilitated specimens significantly. The average ductility increased by 0%, 63% and 35% for specimens RC1, RC2 and RC3 with respect to their corresponding control specimens. The average peak load increased by 31%, 28% and 69% in the pull direction and by 33%, 31% and 61% in the push direction for specimens RC1, RC2 and RC3 with respect to their corresponding control specimens.

Table 1. Peak test load and ductility for positive and negative direction.

Specimen	Peak load (kN)		Average peak load (kN)	Displacement at the yield point (mm)		Displacement at 20% drop of peak load (mm)		Ductility factor		Average Ductility factor
	pull(+)	push(-)		pull(+)	push(-)	pull(+)	push(-)	pull(+)	push(-)	
C1	36.4	41.9	39.2	13.6	18.4	72.0	72.0	5.3	3.9	4.6
C2	31.3	37.1	34.2	14.4	18.4	54.0	54.0	3.8	2.9	3.3
C3	21.1	36.3	28.7	15.2	21.6	25.8	54.0	1.7	2.5	2.1
RC1	47.6	55.8	51.7	13.8	18.7	72.0	72.0	5.2	3.8	4.5
RC2	40.0	48.6	44.3	13.9	18.9	54.0	54.0	3.9	2.8	3.4
RC3	35.6	58.5	47.1	13.6	19.1	38.4	54.0	2.8	2.8	2.8

3.3 Energy dissipation capacity and stiffness degradation

The comparison of cumulative hysteresis energy dissipation and degradation of peak-to-peak secant stiffness for all specimens is shown in **Figure 10**a and **Figure 10**b respectively. The energy dissipated from the beginning of the test till ±4.5% drift ratio for the control specimens C1, C2 and C3 and rehabilitated specimens RC1, RC2 and RC3 was 17.3, 7.8, 5.7, 23.4, 20.6 and 14.1 kN.m, respectively. As shown in **Figure 10**a, the rehabilitated specimens dissipated more energy with respect to their corresponding control specimens up to 35%, 160% and 147% for the rehabilitated specimens RC1, RC2 and RC3 respectively. As shown in **Figure 10**b, the initial stiffness of the rehabilitated specimen are very consistent and had a lower rate of cyclic stiffness degradation with respect to their corresponding control specimens.
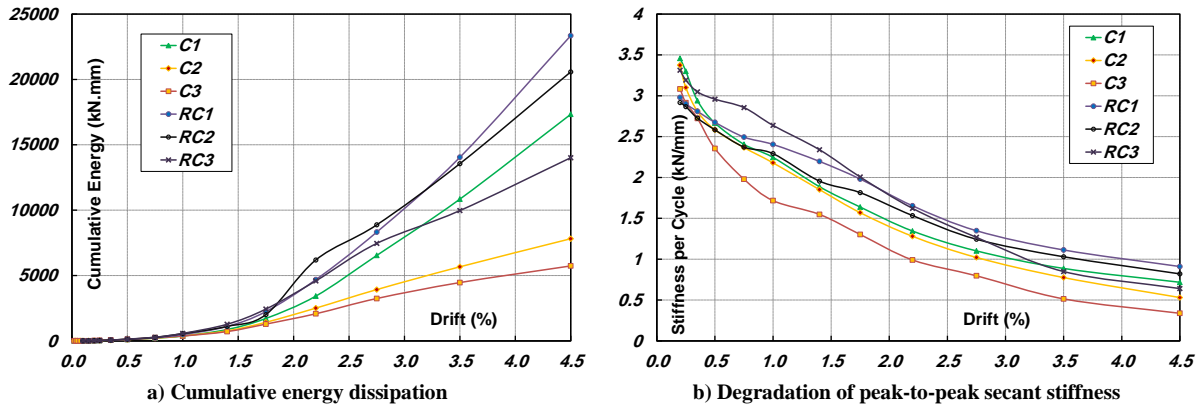

Figure 10. Comparison of cumulative energy dissipation and degradation of peak-to-peak secant stiffness.

4 CONCLUSIONS

In the current study a practical technique for rehabilitation of seismically and non-seismically detailed external RC beam-column joints damaged due to cyclic loading was investigated. Based on the observations and the experimental results of this study, the key findings of the experimental program are:

1. The non-seismically detailed control specimens showed a high rate of strength and stiffness degradation when compared to their rehabilitated equivalents, due to unconfined joints and inadequate anchorage length of the beam bottom bars.

2. The general behaviour mode for all rehabilitated specimens was flexural yielding in the beam outside the joint panel at the edge of joint enlargement.

3. The proposed rehabilitation method was shown to significantly enhance the seismic capacity of the joints, in terms of strength, stiffness, energy dissipation and ductility capacity.

4. Pinching of the load-displacement hysteretic curve for the rehabilitated specimens was significantly decreased and the energy dissipation capacity was increased up to 35%, 160% and 147% for specimens RC1, RC2 and RC3 with respect to their corresponding control specimens.

5. The average maximum peak loads for the positive and negative loading directions for the rehabilitated specimens was increased by 32%, 30% and 64% for specimens RC1, RC2 and RC3 with respect to the corresponding control specimens.

5 ACKNOWLEDGMENTS

experimental works.

REFERENCES

ACI Committee 318M-11. 2011. *Building Code Requirements for Structural Concrete (ACI 318M-11)* and Commentary. American Concrete Institute, Farmington Hills, Michigan, USA.

ACI Committee 374.1-05. 2005. *Acceptance Criteria for Moment Frames Based on Structural Testing and Commentary (ACI 374.1–05)*. American Concrete Institute, Farmington Hills, Michigan, USA.

Cheung, P.C., Paulay, T., and Park, R. 1991. Mechanisms of Slab Contributions in Beam-Column Subassemblages. *Aci Special Publication on Beam-Column Joints*.

Dogangun, A. 2004. Performance of reinforced concrete buildings during the May 1, 2003 Bingol Earthquake in Turkey. *Eng Struct* 26(6): 841-856.

Elwood, K.J., Matamoros, A.B., Wallace, J.W., Lehman, D.E., Heintz, J.A., Mitchell, A.D., Moore, M.A., Valley, M.T., Lowes, L.N., and Comartin, C.D. 2007. Update to ASCE/SEI 41 concrete provisions. *Earthquake Spectra* 23(3): 493-523.

Elwood, K.J., Pampanin, S., and Kam, W.E. 2012. 22 February 2011 Christchurch Earthquake and Implications for the Design of Concrete Structures. *In Proceedings of the International Symposium on Engineering Lessons Learned from the 2011 Great East Japan Earthquake*, Tokyo, Japan.

Engindeniz, M., Kahn, L.F., and Zureick, A.H. 2005. Repair and strengthening of reinforced concrete beam-column joints: State of the art. *Aci Struct J* 102(2): 187-197.

FEMA 308. 1998. *Repair of Earthquake Damaged Concrete and Masonry Wall Buildings*. Federal Emergency Management Agency, prepared by the Applied Technology Council (ATC-43 Project), Washington, D.C.

Kam, W.E., Pampanin, S., and Elwood, K.J. 2011. Seismic Performance of Reinforced Concrete Buildings in the 22 February Christchurch (Lyttelton) Earthquake. *New Zealand Society for Earthquake Engineering Bulletin* 44(4): 239-278.

Korkmaz, S.Z., and Korkmaz, H.H. 2013. The structural damages and collapse types in Turkey, observed after the recent earthquake. *Advanced Materials Research* 747(1): 437-440.

Leon, R., and Jirsa, J.O. 1986. Bidirectional Loading of R.C. Beam-Column Joints. *Earthquake Spectra* 2(3): 537-564.

Norton, J.A., King, A.B., Bull, D.K., Chapman, H.E., McVerry, G.H., Larkin, T.J., and Spring, K.C. 1994. Northridge Earthquake Reconnaissance Report (Report of the NZNSEE Reconnaissance Team on the 17 January 1994 Northridge, Los Angeles Earthquake). *New Zealand Society for Earthquake Engineering Bulletin* 27(4): 235-344.

Ozturk, M. 2013. Field Reconnaissance of the October 23, 2011 Van, Turkey Earthquake (Mw=7.2): Lessons Learned from Structural Damages. *Journal of Performance of Constructed Facilities*.

Park, R. 2002. A Summary of Results of Simulated Seismic Load Tests on Reinforced Concrete Beam-Column Joints, Beams and Columns with Substandard Reinforcing Details. *Journal of Earthquake Engineering* 06(02): 147-174.

Park, R., and Paulay, T. 1975. *Reinforced Concrete Structures*. John Wiley & Sons, New York.

Paulay, T., and Priestley, M.J.N. 1992. *Seismic Design of Reinforced Concrete and Masonry Buildings*. John Wiley & Sons, New York.

Shafaei, J., Hosseini, A., and Marefat, M.S. 2013. Seismic Retrofitting of non-Seismic Detailing External RC Beam-Column Joints by Joint Enlargement Using Steel Angles. *In The Fourth International Conference on Concrete and Development*, Tehran, Iran, April 28-30, Paper No. C&D4-04, Available from.http://www.bhrc.ac.ir/

Shafaei, J., Hosseini, A., Marefat, M.S., and Aerzyton, A. 2012. Experimental Evaluation of New Technique for Seismic Retrofitting of External R Beam-Column Joint with Non Seismic Detailing. *In 15th World Conference on Earthquake Engineering*, Lisbon, Portugal, September 24-28, Paper No. WCEE2012_2263, Available from.http://www.iitk.ac.in/nicee/wcee/article/WCEE2012_2263.pdf

Sugano, S. 1996. State of the art in Techniques for Rehabilitation of Buildings. In *11th World Conference on Earthquake Engineering*, Acapulco, Mexico.